Data-driven adaptive dynamic coordination of damping controllers

Francisco Zelaya-Arrazabal[†], Jingzi Liu[†], Jin Zhao[†], Héctor Pulgar-Painemal[†], Fangxing Li[†], Horacio Silva-Saravia*

† Department of Electrical Engineering and Computer Science. University of Tennessee, Knoxville.

{fzelayaa, jliu}@vols.utk.edu, {jzhao44, hpulgar, fli6}@utk.edu,

* Electric Power Group, LLC, Pasadena, CA.

silva-saravia@electricpowergroup.com

Abstract—This paper proposes a data-driven adaptive coordination of damping controllers to enhance power system stability. The coordination uses wide-area frequency measurements to select the switching status (on/off) of damping controllers (DC) enabled in electronically-interfaced resources (EIR). This is done by using the total action (TA), a dynamic performance measure of the oscillation energy related to the synchronous generators; and deep neural networks (DNNs), a powerful learning algorithm capable of providing accurate model regression between the grid measurements and the TA. The concept is tested in the Western North America Power System (wNAPS) and compared with a model-based approach for coordination of damping controllers. These are the first results of an extensive research related to coordination of DC-EIR, showing good adaptability and performance to different fault locations across the grid.

Index Terms—Wide area damping control, electromechanical oscillations, small-signal stability, renewable energy resources, deep neural networks.

I. INTRODUCTION

In the last decades, non-conventional renewable resources (NCRS) have significantly increased their share in the generation mix of the power grids around the world. This has led to many changes in the system dynamics, increasing frequency instabilities and the appearance of poorly damped oscillatory modes [1]. These problems have also been exacerbated with the decommissioning of traditional synchronous generators (SG), which decreases not only the system inertia but also the number of power system stabilizers (PSS) in the grid.

Traditionally, local and inter-area oscillations have been tackled by PSS; however, with the appearance of phasor measurements units (PMU) and EIR, many applications for damping controllers have been proposed in the last decade [2], [3]. Although these new advances are promising, the coordination of them is a crucial topic that still needs to be solved. The term coordination has been used extensively in the literature, but with a different meaning from that used in this work. In the early 80s, the coordination of controllers was considered as the selection of location and off-line parameter adjustment of multiple PSS or flexible a.c. transmission systems [4]. With the increase in the number of controllers, constrained optimization and robust control techniques were used in the

This work was supported in part by the National Science Foundation (NSF) under Grant No. 2033910, and in part by CURENT, which is an NSF Engineering Research Center funded by NSF and the Department of Energy under NSF Award EEC-1041877.

coordinated tuning of DC [5]-[7]. However, the main concerns with these approaches were the use of arbitrary functions that lack physical interpretation, the need for expert intervention to define a targeted oscillation mode, and lack of adaptability to specific faults, operating conditions and topology changes. To deal with these challenges, some of the authors proposed the concept of adaptive dynamic coordination of DC [8]. This is based on the oscillation energy (OE) and TA [9], new dynamic performance measurements, with physical interpretation, that have proven to be suitable for systems with multiple dominant modes. The adaptive coordination provides switching signals (on/off) to all DC depending on a particular disturbance, enabling them to tackle only excited modes. However, this model-based approach requires previous computation and storage of several parameters, that may or may not be used depending on the operating conditions, which increases the off-line computational cost and the online activation time of the actuators. We are now proposing a datadriven adaptive coordination that overcomes those difficulties. This paper shows the first results of research that will use the main advantages of data science to propose control structures with adaptable coordination to faults, operating conditions, and topology changes. In this work, the online coordination of several DC-EIR is done by taking advantage of deep learning theory, in specific, DNN as model regression and classifier, which has shown good results solving power system problems [11]–[13]. The main contributions of this paper are: 1) the data-driven adaptive coordination, a framework to use widearea frequency measurements for optimal online coordination of damping controllers; and 2) a 2-level hierarchical control based on DNN—this structure provides efficient and accurate coordination of controllers with adaptability to different fault locations. The paper is structured as follows: Section II presents the concepts of OE and TA, Section III describes the model-based adaptive dynamic coordination, while Section IV describes the proposed data-driven adaptive dynamic coordination. The results of the proposed coordination in the wNAPS test system and the conclusions are shown in section

II. OSCILLATION ENERGY AND TOTAL ACTION

The OE and TA are concepts related with the physical description of the power grid. Both of them are associated

with the energy related to SG oscillations after a disturbance [9]. Due to this physical nature, these concepts are attractive as dynamic performance indices to quantify the dynamic response of the power grid.

A. Oscillation Energy

The OE for a system with p SGs, is given by the sum of its individual energy:

$$E(t) = \sum_{j=1}^{p} H_j \omega_s \Delta \omega_j^2(t)$$
 (1)

where the subscript j represents the j-th SG, $w_s = 120\pi$ is the synchronous speed in rad/s, Δw_j is the speed deviation in p.u. and H_j the inertia constant in s.

B. Total Action

The action is a physical concept that describes the changes of a system over time, defined in this case as the time integral of the OE from $t_0 = 0$ to some time τ ,

$$S(\tau) = \int_0^{\tau} E(t) dt \tag{2}$$

Furthermore, if a stable system is considered, the TA can be defined as:

$$S_{\infty} = \lim_{\tau \to \infty} S(\tau) \tag{3}$$

This last expression considers the entire action of the system after a disturbance, and it can be used to assess and compare the dynamic response due to different conditions.

III. MODEL-BASED ADAPTIVE DYNAMIC COORDINATION (MBADC)

The dynamic coordination of DC is a novel control scheme, recently proposed [8], that aims at increasing oscillation damping by turning on/off available DC-EIR based on current conditions and disturbances. The scheme solves a binary integer programming problem to obtain the optimal switching combination that minimizes S_{∞} . Due to the formulation complexity, a suboptimal solution was achieved by using a linearized power system model. Then, the binary problem was solved through linear sensitivities of the TA. The scheme is briefly described below.

A. Dynamic coordination based on total action sensitivities

Consider a linearized power system with p SGs, m DC-EIR, and n states. The system is given by $\dot{x}=Ax+Bu$, $x(t_0)=x_0$ where $A\in\mathbb{R}^{n\times n};\ x,x_0\in\mathbb{R}^n;\ B\in\mathbb{R}^{n\times m};$ and $u\in\mathbb{R}^m$. Consequently, a state feedback controller with $u=Q_q\Theta Cx$ can be proposed. In closed loop, the system is represented as $\dot{x}=A_qx,\ A_q=(A+BQ_q\Theta C)$, where $\Theta=diag\{\theta_1,...;\theta_k,...\theta_m\}$ is the matrix of damping controller gains, $Q_q=diag\{q_1,q_k,...,q_m\}$ is the switching matrix, and q_k is the signal that activates or deactivates the k-th damping controller. Now, for a given switching combination of DC, consider the similarity transformation $\Lambda_q=M_q^{-1}A_qM_q=diag\{\lambda_{qi}\}$ where λ_{qi} is the i-th eigenvalue and M_q is the matrix of right eigenvectors. The state space model

is transformed to $\dot{z}=\Lambda_q z,\ z_0=M_q^{-1}x_0$ and $z=M_q^{-1}x.$ Thus, the OE for this system becomes [8]:

$$E(t) = \sum_{j=1}^{p} H_j \omega_s \Delta \omega_j^2(t) = x^T \mathbf{H} w_s x = \frac{1}{2} z^T \mathbf{G} z \qquad (4)$$

where **H** is the inertia matrix in s, with only nonzero elements in the diagonal terms, $\mathbf{H}_{ii} \forall i \in \Omega_w$, with Ω_w being the set of speed indices of SG; and matrix $\mathbf{G} = M^T 2 \mathbf{H} w_s M$ is an equivalent transform inertia matrix. In addition, the TA becomes [8]:

$$S_{\infty} = \lim_{\tau \to \infty} = -\frac{1}{2} \sum_{i=1}^{n} \sum_{j=1}^{n} \frac{z_{0i} z_{0j} g_{ij}}{\lambda_i + \lambda_j}$$
 (5)

Once the OE and TA have been defined for the linearized power system model, an approximated solution to the coordination problem is obtained by relaxing the switching variables $q_k \in \{0,1\} \ \forall \ k \in \{1,2,...,m\}$ and varying them in the range $[0,1] \in \mathbb{R}$, such that the new $\hat{q_k} \in \mathbb{R}$ is a continuous variable, which allows to solve the problem by a first order Taylor expansion of S_{∞} around an initial switching condition q_{k0} :

$$\Delta S_{\infty} \approx \Delta S_{\infty}(\Delta \hat{q}_{1}) + \Delta S_{\infty}(\Delta \hat{q}_{2}) + \dots + \Delta S_{\infty}(\Delta \hat{q}_{m})$$

$$\approx \frac{\partial S_{\infty}}{\partial \hat{q}_{1}} \Delta \hat{q}_{1} + \frac{\partial S_{\infty}}{\partial \hat{q}_{2}} \Delta \hat{q}_{2} + \dots + \frac{\partial S_{\infty}}{\partial \hat{q}_{m}} \Delta \hat{q}_{m}$$
(6)

The variable \hat{q}_k can be seen as a per-unit scaling of the k-th DC gain. The partial derivatives of Eq. 6 are called total action sensitivities (TAS) and are determined by computing the system eigenvalues, eigenvectors and its derivatives [9]. Furthermore, for a given initial disturbance, $\frac{\partial S_\infty}{\partial q_m^2} > 0$ means that a gain increment of the actuator k would worsen the dynamic performance, while $\frac{\partial S_\infty}{\partial q_m^2} < 0$ means a gain increment of the actuator k would enhance the dynamic performance. Finally, Eq. 6 is used to minimize the TA by looking at the independent effect of each switching signal for a given disturbance. The on/off switching logic for the k-th damping controller becomes: Switch on $\{q_k: 0 \to 1 \Longleftrightarrow \frac{\partial S_\infty}{\partial q_k}|_{\hat{q_k}} < 0\}$ and Switch off $\{q_k: 1 \to 0 \Longleftrightarrow \frac{\partial S_\infty}{\partial q_k}|_{\hat{q_k}} > 0\}$.

B. Implementation

The implementation of this controller requires two stages, the off-line stage and the online stage. The first stage provides the necessary information to calculate the TAS of all damping controllers for a defined set of disturbances. The outcome is a collection of data that includes the eigenvalues, eigenvectors, its corresponding derivatives and the predefined initial switching condition q_{k0} .

The second stage is the implementation of a 2-level hierarchical control: 1st level decentralized control that corresponds to the traditional local damping controller, and 2nd level centralized control which corresponds to the coordination of controllers through the TAS. Fig. 1 shows the structure of this controller, which includes the red and blue boxes. Latter, it will be showed that the proposed scheme of this paper only requires the red box.

IV. DATA-DRIVEN ADAPTIVE DYNAMIC COORDINATION (DDADC)

The main challenge in the coordination of damping controllers is to find the best switching combination for some initial state right after the disturbance. This paper proposes an adaptive data-driven approach by using DNNs. This approach does not require to store previously collected information, and it is able to act online, immediately after the disturbance.

A. Dynamic coordination based on data

Consider a system with m DC-EIR and z switching combinations. The coordination problem can be tackled by obtaining the multivariate function $\hat{S}_{\infty}(y_0,\Gamma_i)$, which is an approximation of S_{∞} . Here, $y_0 \in \mathbb{R}^n$ is the vector of initial states, n the number of states, $\Gamma_i = [\gamma_1, \gamma_i, ..., \gamma_m] \in \Gamma_{\mathbf{z}}$ is the vector of switching status, and $\Gamma_{\mathbf{z}}$ is the set of all possible switching combinations. This multivariate function is given by a DNN, used as a model regression, which is able to learn the relation between the system initial states, the DC-EIR combinations, and its corresponding TA. Once the learning algorithm is trained, the next step is to determine the best switching status Γ^* that minimizes \hat{S}_{∞} for any given initial states y_0 . Thus,

$$\Gamma^* = \underset{\Gamma_i \in \mathbf{\Gamma_z}}{\arg \min} \, \hat{S}_{\infty}(y_0, \Gamma_i) \tag{7}$$

This is a binary integer programming problem and its complexity depends on the value of m. For a small value of m, this can be solved by taking advantage of the DNN which is able to quickly provide the results of all the possible switching combinations. Thus, the switching status is obtained by exhaustive search, selecting the one that produces the smallest \hat{S}_{∞} . For larger values of m, more effective optimization techniques will be explored in the future. As a new-generation advanced modeling tool, DNN exhibits the powerful ability to extract the complex features of the relationship between the input and output data. Based on the multiple hidden layers, DNN shows higher capabilities to capture and model system nonlinearities. This approach does not require a previous defined on/off status of the DC. The EIR could be focused on its main roles inside the power grid and be activated with a DC just when the grid requires it.

B. Proposed structure

Similar to the MBADC, this controller is formed by a 2-level hierarchical scheme: 1st level is the decentralized control that corresponds to the traditional local damping controller, and 2nd level is the centralized control which corresponds to the coordination of controllers through deep learning techniques. Recalling Fig. 1, this scheme has the same structure as the model-based controller, but without the section inside the blue dotted box. This approach does not require previously stored information about the grid. Although this structure also requires an off-line training of the DNN, based on non-linear dynamic simulations, the well-trained DNN achieves model-free application. The DDADC will provide rapid computation speed and better adaptivity than model-based approaches.

C. Implementation

The DDADC was implemented using DIgSILENT-PowerFactory 2018 [15], a very well-known commercial software used for power system analysis. The implementation is divided in the following parts:

1) **Data collection:** The necessary data must reflect the required control adaptability. In this work, the coordination considers adaptability to different fault conditions. Future work will include adaptability to operating conditions and topology changes.

A relation between different faults and the intrinsic response of the grid due to these disturbances is sought. Recalling Eqs. 1 and 3, the OE and TA are functions that depend on the SG frequency. Thus, after a disturbance, the frequency at the SG buses is a suitable variable to train the DNN. However, the actual frequency in the grid depends on the demand and generation balance, which is constantly changing. To deal with this, a better approach is to use the frequency deviation of SG buses with respect to a reference bus. This will reflect similar frequency deviations even with different pre-fault frequency conditions in the grid. In that sense, the frequency deviation $\Delta\omega_{sq}$ will be used as y_0 on Eq. 7. Several non-linear dynamic simulations for different fault scenarios are performed, saving a collection Φ which contains the TA, the snapshot of the system states and the switching condition of each DC-EIR in each simulation. The specific steps for data collection are described on Algorithm 1.

Algorithm 1 Data collection

```
1: Define v_i \ \forall \ j \in \Upsilon = \{1, ..., l\}  \triangleright Vector of disturbances
 2: Define \Gamma_i \ \forall \ i \in \Gamma_{\mathbf{z}} = \{1, ..., z\}
                                                          ▷ Switching comb.
 3: for each v_j \in \Upsilon = \{1, ..., l\} do
 4:
          for each \Gamma_i \in \Gamma_z = \{1, ..., z\} do
               Run dynamic simulation
 5:
 6:
               if Time = Clearing \ time then
                    y_{0li} = \Delta \omega_{sq}
 7:
 8:
               if Time = end then
                    Calculate total action S_{\infty li}
 9:
                    Save the collection \Phi:
10:
                    \{v_{ji}, y_{0ji}, \Gamma_{ji}, S_{\infty ji}\}
11:
```

2) Training DNN: Although for most of the simulated scenarios, the system is stable, some of them can lead to instability. While the TA can be determined for the stable scenarios, this is undetermined for the unstable ones. To deal with this, two separate DNN models are used. The first one is a classification DNN model (C-DNN) used to discriminate between the convergent and non-convergent cases. The second is a regression DNN model (R-DNN) used to calculate the corresponding TA value for the given input data.

To get the best performance and avoid any biases, cross validation is used to determine the network configuration. The whole samples are separated into 10 folders, with a ratio of 3:7. Three folders are validation data-set and the other seven are training data-set. Now, consider 10 different rounds of this data

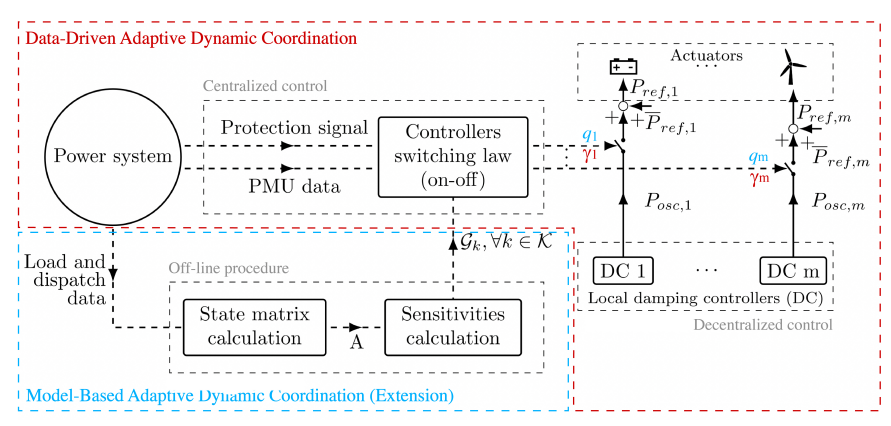


Fig. 1: Controller Structure. Note: the model-based coordination considers the entire structure, while the data-driven coordination only requires the structure inside the red box.

configuration. In each round, the folders of validation set and training set will be forward rolled; e.g in round one, folders 1 to 3 will be the validation set while the other 7 will be the training set; then in round two, folders 2 to 4 will be the validation set, while folders 1 and 5 to 10 will the training set. After each round, the accuracy between the estimated value and ground truth of the validation set will be recorded. This will be used to compute the average accuracy for further comparison. Also, to guarantee a better convergence, each value y_{0ji} in the data collection it is normalized by its related standard deviation and mean.

The training process takes the following considerations regarding the output data. For the C-DNN, converged cases are label as class 1, while diverged cases as class 0. For the R-DNN, first the diverged cases are discarded, then the model is trained with the actual TA value of the converged cases. The optimal DNN structure was obtained by using the control variate method, aiming to reduce the error in the output. A well-trained DNN relies on its structure, which depends on the number of hidden layers and neurons, and the activation function; this last one could add a nonlinear factor to simulate more complex relationships. In this paper and for both cases, the final structure consider 37 neurons for the input layer, 4 hidden layers of 5000 neurons and one neuron for the output layer; also, the ReLU function was used as activation function. Finally, stochastic gradient descent was used to ensure an optimal solution for both DNN. The training process was done using TensorFlow library in Python obtaining a network configuration with more than 97 % accuracy.

3) Control design: Once the DNNs are trained, the control is designed in DIgSILENT-PowerFactory by taking advantage of its direct communication with MATLAB [15]. In specific, the data collection stage and the control scheme were done using DIgSILENT programming language (DPL) and DIgSILENT simulation language (DSL), respectively. For the sake of brevity, only the control design is discussed in this document. The control uses several composite model frames, the number of them depends on the amount of measurement and actuators; all of them are nested in one global frame.

The authors classified these composite model frames in three types. 1) Measurement and MATLAB communication frame: this is used to collect all the frequency measurements from the grid and transmit them to MATLAB, such that the best switching combination can be obtained. 2) Frequency control frame: this one is the decentralized control of each DC-EIR. 3) Global DDADC frame: this is the centralized control, which is a nested frame that considers the first two types. This implementation considers the two following levels:

- a) 1st level control (decentralized control): The DC is connected by a switch to an EIR, modeled as a controlled voltage source [8]. This provides a supplementary reference signal of active power $(P_{osc,k})$ in addition to a main reference signal with slower dynamics $(\overline{P}_{ref,k})$, such as power dispatch or secondary frequency control. Thus, the reference power is expressed in terms of the switching signal determined by the centralized control, as $P_{ref,i} = P_{osc,i} \cdot \gamma_i + P_{ref,i}$ for the DDADC. Note that for the MBADC this is changed to $P_{ref,k} = P_{osc,k} \cdot q_k + P_{ref,k}$.
- b) 2nd level control (centralized control): This corresponds to the solution of the data-driven dynamic coordination. After the fault is cleared, a protection signal at time stamp t_0 is sent to the centralized control such that the frequency measurements at the generator buses are used to compute $y_0 = \Delta \omega_{sg}$. This vector together with each $\Gamma_i \in \Gamma_{\mathbf{z}}$ is used to feed the DNN to compute $\hat{\mathbf{S}}_{\infty}$, the vector of all estimated TA for each possible controller combination. Then, Γ^* is obtained as the controller combination that produces the smallest TA. Consequently, the switching signal $\gamma_i \in \{0,1\}$ is sent by the centralized control to each of the DC-EIR to determine whether it is activated or not.
- 4) PowerFactory MATLAB communication:
 PowerFactory-DSL does not handle well large algebraic structures as weighting matrices and biases vectors, or activation functions required by the DNN. Furthermore, implementing a search algorithm with conditional sentences and for loops is not straightforward as it could be in other programming languages. Due to this, the authors took advantage of the communication environment provided by

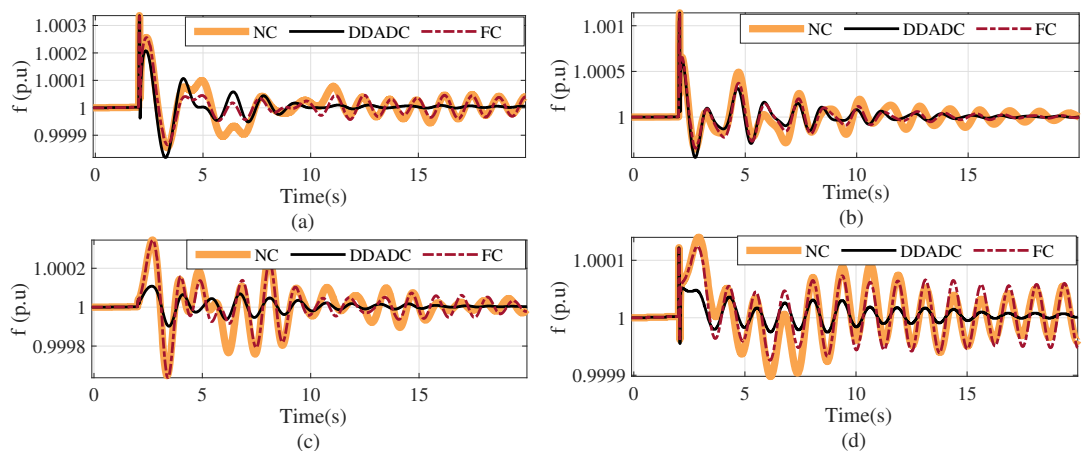


Fig. 2: Frequency comparison for different control scenarios. Frequency at bus: (a) 117, (b) 14, (c) 161, and (d) 69.

PowerFactory. This uses a "MATLAB M-file model" DSL block (BlkDef) to exchange real-time data with MATLAB. The measured variables on PowerFactory are sent through this block to MATLAB, where a function is used to execute the DNN and the search algorithm. The communication is carried on through the entire dynamic simulation, however, one can define a time window or a signal that allows executing the DNN and the searching algorithm only when it is required. In our case, this will be an activation signal right after the disturbance is cleared at t_0 . Once the switching combination is obtained, this is retransmitted through the same DSL block and feed to each decentralized DC-EIR.

5) DDADC remarks: The C-DNN and R-DNN provided high accuracy results; furthermore, the DDADC reduced the TA in each of the test cases. However, any data-driven approach raise concerns, since the outputs could be incorrect in cases where the input data deviates too much from the training set. In those cases, it is important to consider an approach that allows aborting the coordination and return to a safe operation. One approach could be to return to a fixed coordination that only considers the PSSs tuned to damp the most common modes. However, in any of the selected approaches, it is necessary to determine a new index or approach that allows to identify that the system is becoming unstable. This type of indices and safe coordination will be explored in future works.

V. CASE STUDY

The proposed scheme is tested in the wNAPS, a reduced model of the Western Electricity Coordinating Council (WECC). This test system is formed by 179 transmission buses, 31 SG, 7 DC-EIR, and a hypothetical scenario with 20% wind power penetration. The latter achieved by connecting 11 equivalent DFIG-based wind turbines. A detailed description, network, operational data, and dynamic parameters are found in [8], [16]. Although the chosen operational conditions do not resemble those of the actual WECC system, the model contains modes that mimic the four well-known inter-area modes: "NS mode A", "NS mode B", "BC mode" and "Mon-

tana mode", among others [17], but with an intended more critically undamped behavior for the sake of analysis.

A. Simulated scenarios

Each simulation considers a 3-phase fault to ground at t=2.0s cleared after 3 cycles. The adaptive coordination is activated at the clearing time, providing the coordination after being fed by the frequency measurements across the grid. This does not require a previously stipulated actuator on/off condition, the DC-EIR are immediately activated by the centralized control after the disturbance. Fig. 2 shows the frequency at buses 117, 14, 161, and 69, for a fault on bus 57 and different control scenarios: no DC-EIR (NC), orange curve, the system with DDADC, black curve, and the system with a fixed set of DC-EIR (FC), maroon dashed curve. This last scenario considers the DC-EIR 63, 79, 107, and 140 turned on. It is evident the oscillation reduction with both, the DDADC and the FC, however, the former produces the best reduction across the grid. Fig. 3 shows that the adaptive coordination, black curve, reduces the OE compared with a traditional fixed set of controllers, maroon dashed curve. Furthermore, this is corroborated with the TA $S_{\infty,DDADC} = 0.1619$ and, $S_{\infty,FC} = 0.207$ for the DDADC and FC, respectively, which represents a 38.70% and 21.60% of TA reduction with respect to the system without controllers.

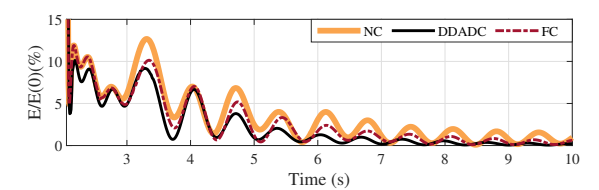


Fig. 3: OE for short-circuit at bus 57.

B. Comparison between MBADC and DDADC.

The proposed coordination was compared with our previous results based on MBADC. Two short-circuits are compared, the first at bus 157, east side of the grid, and the second at bus

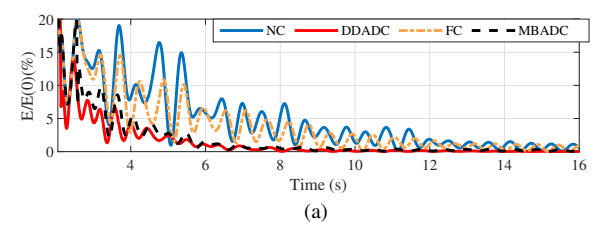
TABLE I: TA reduction comparison

	Short-circuit at bus 157		Short-circuit at bus 69	
Coordination	Total Aciton	Redutcion	Total Aciton	Redutcion
		(%)		(%)
No DC-EIR	1.241	-	0.840	-
Fixed Coordination	0.998	19.60	0.998	-18.79
DDADC	0.328	73.53	0.295	64.87
MBADC	0.500	59.72	0.473	43.65

69, north side. Fig. 4 shows the OE for both short-circuits, the DDADC, red curve, and MBADC, black curve, have similar results, reducing the OE compared with the traditional fixed set of controllers, orange curve. Table I shows the comparison of the reduction in the TA. The biggest reduction of 73.53% is obtained with the proposed DDADC, which means an improvement in the oscillation damping in an optimal sense. For short-circuit at bus 69, the FC, orange curve, worsens the dynamic response of the system, incrementing the OE, and the TA which are a direct consequence of the oscillations increase in the grid. It is common to tune and coordinate PSSs or DCs to specific modes that considers the most common disturbances. However, there are uncommon faults that could be aggravated with those coordinations, similar to this case. Despite that, both DDADC and MBADC are able to reduce the OE, minimizing the TA and improving the damping of the system. This can also be corroborated in Table I. The results show a big improvement in the dynamic response of the system, relying on the optimal use of the DC-EIR. This highlights the novelty in both approaches, providing a new framework to optimize the use of resources like photovoltaic, wind power plants, and any other EIR that have operational and energetic constraints. The DDADC is a suitable approach for getting the most out of EIRs, since the schemes is able to improve the dynamic response of the system by coordinating the DC exactly and only when it is needed.

VI. CONCLUSION

This paper proposes a novel data-driven adaptive coordination of damping controllers, based on TA measurement performance and deep neural networks. The proposed framework uses direct measurements of the system right after a disturbance to feed the coordination scheme and obtain the switching status (on/off) of several DC-EIR. This is a novel approach, that provides an accurate coordination adaptable to any disturbance, without requiring a previously fixed status of the DCs, nor previously storage information. The work provides a framework to improve the dynamic response of the system by using any EIRs in an optimal sense. This makes possible to use resources like solar panels, wind turbines, battery energy storage, and any other EIRs that are subjected to operational and energetic constraints, using them only when needed. The proposal it is implemented in PowerFactory, by using its communication interface with MATLAB and is compared with a model-based approach. The results prove to successfully determine the switching status of the DC-EIR that quickly damp the oscillations in the grid, minimize the TA, and improve the dynamic response of the system.



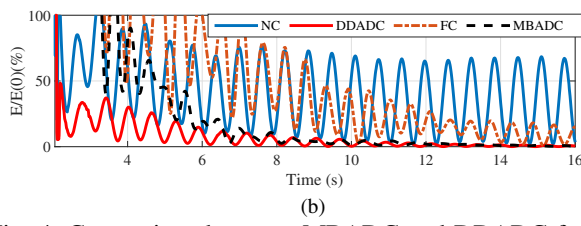


Fig. 4: Comparison between MBADC and DDADC for short-circuit at bus: (a) 157, and (b) 69.

REFERENCES

- Tielens, Pieter, and Dirk Van Hertem. "The relevance of inertia in power systems." Renewable and Sustainable Energy Reviews 55 (2016).
- [2] M. R. Younis and R. Iravani, "Wide-area damping control for inter-area oscillations: A comprehensive review," 2013 IEEE Electrical Power & Energy Conference, 2013, pp. 1-6.
 [3] ZHANG, Xinran, et al. "A review on wide-area damping control to
- [3] ZHANG, Xinran, et al. "A review on wide-area damping control to restrain inter-area low frequency oscillation for large-scale power systems with increasing renewable generation," Renewable and Sustainable Energy Reviews, 2016, vol. 57, p. 45-58.
- [4] F. P. Mello, P. J. Nolan, T. F. Laskowski, and J. M. Undrill, "Coordinated application of stabilizers in multimachine power systems," IEEE Trans. Power App. Syst., vol. PAS-99, no. 3, pp. 892–901, May 1980.
- [5] Pal, Bikash, and Balarko Chaudhuri. Robust control in power systems. Springer Science & Business Media, 2006.
- [6] R. A. Jabr, B. C. Pal, N. Martins, and J. C. R. Ferraz, "Robust and coordinated tuning of power system stabiliser gains using sequential linear programming," IET Gener., Transmiss. Distrib., vol. 4, no. 8, 2010.
- [7] I. Kamwa, G. Trudel, and L. Gerin-Lajoie, "Robust design and coordination of multiple damping controllers using nonlinear constrained optimization" IEEE Trans. Power Syst., vol. 15, no. 3, Aug. 2000.
- [8] H. Silva-Saravia, H. Pulgar-Painemal, D. A. Schoenwald and W. Ju, "Adaptive Coordination of Damping Controllers for Enhanced Power System Stability," in IEEE Open Access Journal of Power and Energy, vol. 7, pp. 265-275, 2020.
- [9] H. Silva-Saravia, Y. Wang, H. Pulgar-Painemal and K. Tomsovic, "Oscillation Energy based sensitivity analysis and control for multi-mode oscillation systems," 2018 IEEE Power and Energy Society General Meeting (PESGM), 2018, pp. 1-5.
- [10] I. Goodfellow, Y. Bengio, and A. Courville, Deep Learning. Cambridge, MA, USA: MIT Press, 2016, pp. 152–231.
- [11] F. Li and Y. Du, "From alpha go to power system AI," IEEE Power Energy Mag., vol. 16, no. 2, pp. 76–84, Mar./Apr. 2018.
- [12] X. Kou et al., "Model-based and data-driven HVAC control strategies for residential demand response," IEEE Open Access J. Power Energy, vol. 8, pp. 186–197, 2021.
- [13] Zhao, Jin, et al. "Deep learning based model-free robust load restoration to enhance bulk system resilience with wind power penetration." IEEE Transactions on Power Systems 37.3 (2021): 1969-1978.
- [14] M. I. Friswell, "Calculation of second and higher order eigenvector derivatives," J. Guid., Control, Dyn., vol. 18, no. 4, pp. 919–921. 1995.
- [15] DIgSILENT PowerFactory User Manual, DigSILENT GmbH, Gomaringe, Germany, 2018.
- [16] Test Cases Library of Sustained Power System Oscillations. Accessed: Jan. 2020. [Online]. Available: http://web.eecs.utk.edu/ kaisun/Oscillation/
- [17] D. Trudnowski, D. Kosterev, and J. Undrill, "PDCI damping control analysis for the Western North American power system," in Proc. IEEE Power Energy Soc. Gen. Meeting, Jul. 2013, pp. 1–5